Barrier To Linearity and Anharmonic Force Field of the Ketenyl Radical†

Andrew C. Simmonett,‡ Nathan J. Stibrich,‡ Brian N. Papas,‡ Henry F. Schaefer III,‡ and Wesley D. Allen*,‡,§

Center for Computational Quantum Chemistry and Department of Chemistry, University of Georgia, Athens, Georgia 30602

Received: March 18, 2009; Revised Manuscript Received: July 26, 2009

The troublesome barrier to linearity of the ketenyl radical (HCCO) is precisely determined using state-of-the-art computations within the focal point approach, by combining complete basis set extrapolation, utilizing the aug-cc-pV*X*Z (*X* = D, T, Q, 5, 6) family of basis sets, with electron correlation treatments as extensive as coupled cluster theory with single, double, triple, and perturbative quadruple excitations [CCSDT(Q)]. Auxiliary terms such as diagonal Born−Oppenheimer corrections (DBOCs) and relativistic contributions are included. To gain a definitive theoretical treatment and to assess the effect of higher-order correlation on the structure of HCCO, we employ a composite approximation (c∼) to all-electron (AE) CCSDT(Q) theory at the complete basis set (CBS) limit for geometry optimizations. A final classical barrier to linearity of 630 ± 30 cm^{-1} is obtained for reaching the $^2\Pi$ Renner−Teller configuration of HCCO from the $^2A''$ ground state. Additionally, we compute fundamental vibrational frequencies and other spectroscopic constants by application of second-order vibrational perturbation theory (VPT2) to the full quartic force field at the AE-CCSD(T)/aug-cc-pCVQZ level. The resulting (ν_1, ν_2, ν_5) fundamental frequencies of (3212, 2025, 483) cm^{-1} agree satisfactorily with the experimental values (3232, 2023, 494) cm^{-1}.

Introduction

The ketenyl (HCCO) radical was long ago recognized as a prevalent component of hydrocarbon flames[1] and is thought to have astrophysical significance as well.[2,3] Thus, it has been the subject of numerous kinetic,[4−12] spectroscopic,[13−22] and theoretical investigations.[2,23−36] The HCCO radical is produced as an intermediate during acetylene combustion by the reaction

$$C_2H_2 + O(^3P) \rightarrow HCCO + H \qquad (1)$$

which has been studied extensively.[7,37−41] The emission of NO_x species from combustion systems is recognized as a contributing factor to acid rain and smog formation,[42] and much research has been dedicated to reducing these emissions. One such strategy is reburning,[43] in which the reduction of HCCO by nitric oxide features prominently.[44] Furthermore, the reactions of ketenyl with nitrogen dioxide

$$\begin{aligned} HCCO + NO_2 &\rightarrow HCNO + CO_2 \\ &\rightarrow HCO + NO + CO \end{aligned} \qquad (2)$$

have recently garnered attention[45,46] due to their involvement in the NO_x cycle.

By analyzing the submillimeter microwave spectrum of HCCO, Endo and Hirota[15] determined that the HCCO radical has a bent ground-state geometry. Two fundamental vibrational frequencies were observed[17,47] for the ground state by laser-induced fluorescence, the CCH bending mode at 494 cm^{-1} and a stretching mode at 2023 cm^{-1}. More recently, the ν_1 CH stretching mode was observed[48] via FTIR emission spectroscopy at 3232 cm^{-1}. In 2003, the photodissociation of ethyl ethynyl ether was shown to be an extremely efficient photolytic route to the HCCO radical, enhancing the feasibility of experimental studies.[49]

The ground state of HCCO was first studied theoretically through configuration interaction (CI) computations by Harding in 1981;[23] the inclusion of correlation is imperative as its effects are pronounced for the properties of this molecule.[25] The ground state of HCCO has a trans-bent geometry and is a $^2A''$ electronic state. At linearity, HCCO is a $^2\Pi$ Renner−Teller molecule, with nondegenerate quadratic force constants for the bending modes that lead to $^2A''$ and $^2A'$ electronic states in C_s symmetry. In particular, the trans-bending mode that leads to the $^2A''$ ground state has a negative force constant associated with it, while the corresponding mode leading to the $^2A'$ state has a positive force constant, making linear HCCO a type (C) Renner−Teller system.[50] Szalay and co-workers have used coupled cluster methods to characterize the $^2A''$ ground state and elucidate the features of the $^2\Pi$ Renner−Teller state.[26,29,31]

Several kinetic experiments have concluded that the C_2H + $O(^3P)$ reaction should proceed through a transition state similar to the $^2A'$ state of HCCO, or one of its vibrationally excited levels.[51−53] A linear transition state has also been investigated for the collisional quenching of $CH(a^4\Sigma^-)$ by CO.[30] While the enthalpy of formation for the $^2A''$ ground state of HCCO has been thoroughly investigated in an important recent paper by Szalay, Tajti, and Stanton,[36] the relative energy of the linear $^2\Pi$ state is still a matter of debate. Experimentally, the barrier to linearity is difficult to determine. Endo and Hirota[15] deduced from pure rotational spectra that the energy barrier should be 3200 cm^{-1} if the unpaired electron is localized on the oxygen or 540 cm^{-1} if localized on the neighboring carbon, preferring the latter choice. The key assumption in their analysis was that the unpaired electron is localized on either the carbon or oxygen

† Part of the "Walter Thiel Festschrift".

* To whom correspondence should be addressed. E-mail: wdallen@uga.edu.
‡ Center for Computational Quantum Chemistry.
§ Department of Chemistry.

10.1021/jp9024365 CCC: $40.75
Published on Web 09/17/2009

TABLE 1: Theoretical and Experimental Barriers to Linearity ΔE (cm^{-1}) for the Ketenyl Radical[a]

method	AO basis	electrons correlated	ΔE
MCSCF/MRCI[b]	DZP	val	981
CASSCF[c]	DZP	val	1609
RCCSD(T)[c]	DZP	val	1428
UHF[d]	DZP		105
	TZ2P		126
MBPT2[d]	DZP	all	1828
	TZ2P	all	1512
UHF-CCSD[d]	DZP	all	958
	TZ2P	all	786
	cc-pVTZ	all	403
UHF-CCSD(T)[d]	DZP	all	1302
	TZ2P	all	1096
	cc-pVTZ	all	643
EOMIP-CCSD[d]	TZ2P	all	656
	cc-pVTZ	all	268
RHF-UCCSD[e]	cc-pVQZ	val	509
	cc-pV5Z	val	485
	aug-cc-pVQZ	val	509
	aug-cc-pV5Z	val	489
RHF-UCCSD(T)[f]	cc-pVQZ	val	712
	cc-pCVQZ	all	637
RHF-UCCSD(T)[e]	cc-pV5Z	val	687
	aug-cc-pVQZ	val	712
	aug-cc-pV5Z	val	690
	aug-cc-pCVQZ	all	638
CCSDT(Q)[e]	CBS	all	630
experiment[f]			540/3200
experiment[g]			700−900

[a] The theoretical values are classical barriers (without ZPVE contributions) not affected by complications due to the Renner−Teller effect. [b] Kim and Shavitt, quoted in ref 29. [c] Reference 33. [d] References 26 and 29. [e] This research. [f] Reference 15. [g] Reference 34.

atom, which allowed them to assume that the spin−orbit coupling for HCCO is either that of atomic carbon or atomic oxygen. More recently, Schäfer-Bung et al.[34] measured the photoelectron spectrum of the $HCCO^-$ anion. By constructing theoretical models of this spectrum, aided in part by geometries from UHF-UCCSD(T) computations (unrestricted coupled cluster with singles, doubles, and perturbative triples), the group suggested that the barrier to linearity for HCCO lies between 700 and 900 cm^{-1}.

As shown in Table 1, theoretical determinations[26,29,33,34] of the barrier to linearity have varied considerably, ranging all the way from 105 (UHF/DZP) to 1828 cm^{-1} (MBPT2/DZP) due in large part to the strong dependence of ketenyl radical computations on both electron correlation and the atomic orbital basis set. With MRCI computations using a DZP basis set, Kim and Shavitt (quoted in ref 29) predicted the barrier to be 981 cm^{-1}. Szalay et al.[29,31] subsequently used EOMIP-CCSD theory (equation of motion ionization potential CCSD) with a TZ2P basis to determine a somewhat larger barrier of 1175 cm^{-1}. To overcome sensitivities to the level of theory, in this paper, we investigate the barrier to linearity of HCCO using large correlation-consistent basis sets and coupled cluster theory beyond triple excitations. Furthermore, we compute a full internal coordinate quartic force field, from which spectroscopic properties for any isotopologue of HCCO can be extracted.

Methods

This study employs a number of ab initio theories, including restricted open-shell Hartree−Fock (ROHF),[54] second-order Z-averaged perturbation theory (ZAPT2),[55] coupled cluster with single and double excitations (CCSD),[56−59] CCSD with perturbative triple excitations [CCSD(T)],[60−63] coupled cluster with full triple excitations (CCSDT),[64−67] and the full CCSDT model with a perturbative treatment of connected quadruple excitations [CCSDT(Q)].[68,69] These computations, detailed below, were executed with the robust augmented correlation-consistent polarized valence family of basis sets, aug-cc-pVXZ (X = D, T, Q, 5, 6)[70−72] and the associated core−valence augmented set, aug-cc-pCVQZ.[73,74]

The full quartic force field for the bent $^2A''$ ground state of HCCO was computed at the highly accurate all-electron (AE) CCSD(T) level using the large core−valence polarized, quadruple-ζ augmented basis set aug-cc-pCVQZ.[73,74] The reference wave function was a ROHF determinant, and the coupled cluster formalism was fully unrestricted, as signified by ROHF-UCCSD(T) or, more compactly, by ROCCSD(T). For the C and O atoms, the aug-cc-pCVQZ basis is a [16s10p6d4f2g/9s8p6d4f2g] set, and for HCCO, it comprises 373 contracted Gaussian functions. The equilibrium geometry was obtained by analytic energy derivatives.[62,75,76] To obtain accurate fundamental frequencies, anharmonic contributions were computed from the third and fourth derivatives of the molecular energy with respect to nuclear coordinates. These higher-order derivatives were determined by numerical differentiation of tightly converged energies on a grid of displaced geometries. The internal coordinates were chosen as

$$
\begin{aligned}
S_1 &= r(\mathrm{H-C}) \\
S_2 &= r(\mathrm{C-C}) \\
S_3 &= r(\mathrm{C-O}) \\
S_4 &= \theta(\mathrm{H-C-C}) \\
S_5 &= \alpha_x(\mathrm{H-C-C-O}) = \sin[\theta(\mathrm{C-C-O})]\cos(\tau) \\
S_6 &= \alpha_y(\mathrm{H-C-C-O}) = \sin[\theta(\mathrm{C-C-O})]\sin(\tau)
\end{aligned}
$$

where r is the bond length between the specified connected atoms, θ is a valence bond angle, and τ is the H−C−C−O torsional angle. The linear bending coordinates α_x and α_y avert complications arising from the nearly linear CCO bond angle and were shown to be very useful in a study of the geometrically similar HNCO molecule.[77] The determination of the full quartic force field required 263 energies at displaced geometries, with each converged to at least $10^{-11}E_h$. Vibrational anharmonicities were computed by application of second-order perturbation theory[77−84] (VPT2) to the quartic force field. The MATHEMATICA[85] program INTDIF2005[86,87] was used to compute the force constants in internal coordinates, while INTDER2005[88−92] was used to perform the nonlinear transformation of the force constants to the Cartesian space, and the ANHARM[91,93] program provided the VPT2 analysis.

The geometry, particularly the HCC bond angle, and the barrier to linearity have proved to depend strongly upon the computational methodology employed; therefore, the present study investigates the importance of connected quadruple excitations within the coupled cluster ansatz. Due to the computational expense of these high-order terms, we introduce a composite (c∼) approximation to CCSDT(Q) theory at the complete basis set (CBS) limit

$$E^{\mathrm{CBS}}_{\mathrm{c\sim CCSDT(Q)}} = E^{\mathrm{CBS}}_{\mathrm{CCSD(T)}} + E^{\mathrm{cc\text{-}pVDZ}}_{\mathrm{CCSDT(Q)}} - E^{\mathrm{cc\text{-}pVDZ}}_{\mathrm{CCSD(T)}} \quad (3)$$

The CBS values are obtained by extrapolating the Hartree−Fock (E_{HF}) and the all-electron correlation energies (E_{Corr}), obtained with the cc-pCVQZ and cc-pCV5Z basis sets, using the functional forms[94,95]

$$E_{HF}(X) = E_{HF}^{\infty} + a(X + 1)e^{-9\sqrt{X}} \quad (4)$$

and

$$E_{Corr}(X) = E_{Corr}^{\infty} + aX^{-3} \quad (5)$$

For HCCO, the cc-pCVQZ and cc-pCV5Z basis sets comprise 282 and 490 basis functions, respectively. This approach, in which basis set error is accounted for at a lower level of theory, has been successful in past studies, albeit with different levels of theory employed.[96−100] Although the inclusion of full quadruple excitations has been shown to provide excellent results, it remains to be seen whether the same improvements can be gained by using CCSDT(Q) theory, which is less computationally demanding than the full quadruples model, partly because of the noniterative computation of the effects of connected quadruple excitations. The geometries of linear and bent HCCO were optimized within the c∼CCSDT(Q)/CBS approximation, with gradients obtained by numerical differentiation of single-point energies, using the geometry optimization routines within the PSI3[101] quantum chemistry suite.

The barrier to linearity was pinpointed by computing a hierarchical series of single-point energies at the c∼CCSDT(Q)/CBS geometries, within the focal point approach of Allen and co-workers.[102−106] For each level of theory up to CCSD(T), the energies were extrapolated to the complete basis set limit using the functional forms of eqs 4 and 5. As an additional test, the Hartree−Fock energies were also extrapolated using the three-point formula[107]

$$E_{HF}(X) = E_{HF}^{\infty} + ae^{-bX} \quad (6)$$

yielding a barrier to linearity within 0.03 kcal mol^{-1} of that obtained using the two-point fit. Although the CCSDT(Q) formalism has recently been extended to general reference functions,[108] our computations were based upon an unrestricted Hartree−Fock (UHF) reference. Given that the full CI limit is closely approximated at this level, the choice of reference wave function is of little importance in the absence of severe spin contamination at the UHF level; nevertheless, we obtained an estimate of the energetic effect of spin contamination using the formula

$$E_{ROCCSDT(Q)} \approx E_{UCCSDT(Q)} + (E_{ROCCSDT} - E_{UCCSDT}) \quad (7)$$

where the subscript ROCCSDT denotes the energy obtained starting from ROHF reference wave functions, while UCCSDT and UCCSDT(Q) denote computations with UHF reference wave functions. Spin contamination is not expected to be a problem, given the expectation value of $\langle \hat{S}^2 \rangle = 0.81$ for the UHF/aug-cc-pVTZ wave function of bent HCCO.

The massively parallel quantum chemistry package (MPQC)[109] allowed for parallel, direct computation of the ZAPT2 energies,[110] which can be evaluated efficiently due to the reduced number of integrals required; this saving is a consequence of the degeneracy of the α and β spin functions, which is lifted in many other open-shell perturbation theory formulations.[55,111−115] Although the ZAPT2 wave function is not a rigorous $\hat{S}^2$ eigenfunction, the energy is free from the direct effects of spin contamination.[55] The CCSD and CCSD(T) computations were performed with the MOLPRO program suite,[116] while the CCSDT energies were determined using the Mainz−Austin−Budapest (MAB) version of the ACESII program suite.[117,118] The string-based MRCC code of Kállay[69,119] provided the CCSDT(Q) results. The MRCC code is a stand-alone program that is capable of computing arbitrary order coupled cluster and configuration interaction energies; the integrals required for this program were generated with MAB-ACESII. The core orbitals were frozen in the computations employing the aug-cc-pV*X*Z basis sets, consistent with the basis set design; core correlation effects were later accounted for in the focal point analysis, with the aug-cc-pCVQZ basis set,[74] by differencing all-electron (AE) and frozen-core (FC) energies:

$$\Delta E_{core} \approx E_{AE\text{-}CCSD(T)}^{aug\text{-}cc\text{-}pCVQZ} - E_{FC\text{-}CCSD(T)}^{aug\text{-}cc\text{-}pCVQZ} \quad (8)$$

To determine the barrier to linearity with even greater precision, a number of auxiliary corrections were considered. Non-Born−Oppenheimer effects were included through the diagonal Born−Oppenheimer correction (DBOC)[120,121] computed at the ROHF/aug-cc-pVTZ level since the DBOC for relative energies changes little with electron correlation.[122−124] Scalar relativistic corrections were included at the CCSD(T)/aug-cc-pCVTZ level using the one-electron Darwin and mass velocity terms,[125] which have been shown to be accurate for systems with first- and second-row atoms.[126−129]

TABLE 2: Equilibrium Bond Lengths r_e (Å), Harmonic Vibrational Frequencies ω_e (cm^{-1}), Anharmonicity Constants $\omega_e x_e$ (cm^{-1}), and Vibration−Rotation Interaction Constants α_e (cm^{-1}) for the Methylidyne and Carbon Monoxide Molecules

	r_e	ω_e	$\omega_e x_e$	α_e
	CH($X\ ^2\Pi$)			
CCSD(T)/aug-cc-pCVQZ	1.1184	2861.5	64.57	0.537
CCSD(T)/CBS[a]	1.1173	2867.8	65.32	0.537
c∼CCSDT(Q)/CBS[a,b]	1.1175	2864.0	68.58	0.537
experiment[c]	1.1198	2860.8	64.44	0.537
	CO ($X\ ^1\Sigma^+$)			
CCSD(T)/aug-cc-pCVQZ	1.1293	2169.8	13.12	0.0174
CCSD(T)/CBS[a]	1.1276	2177.3	13.22	0.0174
c∼CCSDT(Q)/CBS[a,b]	1.1285	2167.5	13.38	0.0176
c∼CCSDTQ/cc-pV6Z[d]	1.1287			
c∼CCSDTQ/CBS[e]	1.1284			
experiment[f]	1.1283	2169.8	13.29	0.0175

[a] This work. Energies extrapolated according to eqs 4 and 5. [b] Composite approximation; see text for details. [c] Reference 132. [d] Composite approach based upon analytic gradient methods from ref 98. [e] Composite approach based upon analytic gradient methods and extrapolation from ref 99. [f] Reference 133.

Results and Discussion

Our analysis of the geometric structure of HCCO begins by calibrating the performance of our c∼CCSDT(Q)/CBS method for the fragments CO ($X\ ^1\Sigma^+$) and CH ($X\ ^2\Pi$). Table 2 shows the spectroscopic constants obtained from our c∼CCSDT(Q)/CBS approach, alongside experimental and other theoretical results. For the spectroscopic constants of the CH molecule, error cancellation leads to very good results at the CCSD(T)/

aug-cc-pCVQZ level of theory; the corresponding errors in (r_e, ω_e) with respect to experiment are just (−0.0014 Å, 0.7 cm^{-1}), but these rise to (0.0025 Å, 7.0 cm^{-1}) at the CCSD(T)/CBS limit. Appending quadruples via the c∼CCSDT(Q)/CBS approximation offers an improvement over the CCSD(T)/CBS results, bringing the deviations from experiment down to (−0.0023 Å, 3.2 cm^{-1}). Similar trends are observed for the more demanding CO molecule; CCSD(T)/aug-cc-pCVQZ theory gives (r_e, ω_e) values that deviate from experiment by (0.0010 Å, 0.0 cm^{-1}), but these differences become (−0.0007 Å, 7.5 cm^{-1}) at the CCSD(T)/CBS limit. Accounting for quadruple excitations through the c∼CCSDT(Q)/CBS method reduces these errors to just (0.0002 Å, −2.3 cm^{-1}). In all cases in Table 2, the experimental and theoretical vibration−rotation interaction constants are in excellent accord.

Theoretical equilibrium geometric parameters for the $^2A''$ and $^2\Pi$ states of HCCO are collected in Tables 3 and 4, respectively; the best structures obtained in this study, at the c∼CCSDT(Q)/CBS level of theory, are depicted in Figures 1 and 2. The geometries of HCCO optimized at the CCSD and CCSD(T) levels are quite sensitive to both basis set and correlation treatment. Coupled cluster theory, truncated at double excitations, tends to overestimate the CCH bond angle by 1−2° and underestimate all of the bond lengths, particularly the C−O bond length, whose CCSD value is nearly 0.01 Å smaller than the corresponding CCSD(T) result. As a measure of the quality of our geometrical parameters with respect to basis set completeness, we optimized the linear geometry with the cc-pCV5Z basis. In general, the bond lengths at the CCSD(T)/aug-cc-pCVQZ level agree to within 0.001 Å compared to those computed with the larger basis set. For the bent $^2A''$ ground-state geometry, note that the CCO bond angle exhibits very little deviation upon basis set change, while the HCC bond angle is harder to converge; the latter has previously been noted for its extremely flat potential energy surface, which makes a small amount of uncertainty in this value relatively unimportant from an energetic standpoint.[29] With the aug-cc-pCVQZ basis, the difference between the CCSD(T) and CCSD values for ∠HCC is −2.0°, while the corresponding change between c∼CCSDT(Q)/CBS and CCSD(T)/aug-cc-pCVQZ is just −0.12°. Overall, the effect of quadruple excitations is less pronounced than the introduction of triple excitations, indicating convergence toward a consistent result. Our final [c∼CCSDT(Q)/CBS] geometric parameters for the equilibrium structure of HCCO($^2A''$) are r_e(HC) = 1.0710 Å, r_e(CC) = 1.2977 Å, r_e(CO) = 1.1712 Å, ∠HCC = 133.70°, and ∠CCO = 169.20°, which should be highly accurate.

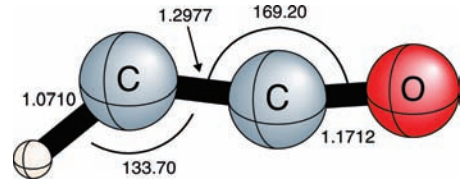

Figure 1. Geometry (Å and deg) of the $^2A''$ ground state of HCCO at the c∼CCSDT(Q)/CBS level of theory. The corresponding parameters from other levels of theory are listed in Table 3.

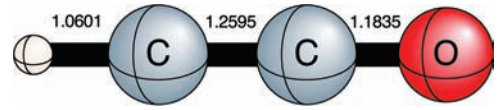

Figure 2. Geometry (Å) of the $^2\Pi$ Renner−Teller state of HCCO at the c∼CCSDT(Q)/CBS level of theory. The corresponding parameters from other levels of theory are listed in Table 4.

Although the geometrical parameters of HCCO are not known experimentally, we can compare the theoretical rotational constants, shown in Table 5, to those extracted from high-resolution microwave spectra. The CCSD(T) rotational constants were corrected for the effects of zero-point vibrational energy using the vibration−rotation interaction constants, presented in Table 6, obtained by applying second-order vibrational perturbation theory (VPT2) to our AE-CCSD(T)/aug-cc-pCVQZ quartic force field. In addition to the vibration−rotation interaction constants, VPT2 yields the vibrational anharmonicity constants in Table 7, from which the fundamental vibrational frequencies in Table 8 were derived.

Table 5 shows the rotational constants for HCCO and DCCO obtained from our theoretical computations, along with those determined from microwave spectra by Endo and Hirota.[15] The quasi-linearity of this system manifests itself in a large A rotational constant, which is difficult to pinpoint both theoretically and experimentally. Endo and Hirota noted difficulties in fitting their spectra due to poorly convergent power series and observed systematic errors between the fitted and observed transition frequencies. To analyze the DCCO microwave spectrum, high orders of centrifugal distortion parameters had to be considered, and the D_K constant had to be constrained to 5000 MHz. The zero-point corrected rotational constants extracted from our CCSD(T)/aug-cc-pCVQZ quartic force field are well within 1% of those measured experimentally, with the

TABLE 3: Equilibrium Geometries (Å and deg) for the $^2A''$ Ground State of HCCO

method	AO basis	electrons correlated	r_e(HC)	r_e(CC)	r_e(CO)	∠HCC	∠CCO
CCSD	cc-pVQZ[a]	val	1.0696	1.2951	1.1639	134.75	169.96
	cc-pV5Z[a]	val	1.0693	1.2942	1.1633	134.90	170.03
	aug-cc-pVQZ[a]	val	1.0700	1.2956	1.1643	134.62	169.89
	aug-cc-pV5Z[a]	val	1.0694	1.2943	1.1634	134.88	170.02
CCSD(T)	cc-pVTZ[b]	val	1.0660	1.2972	1.1728	134.6	169.4
	cc-pVTZ[c]	val	1.0738	1.3072	1.1760	131.92	168.55
	cc-pVQZ[c]	val	1.0729	1.3030	1.1725	132.69	168.92
	cc-pV5Z[a]	val	1.0727	1.3021	1.1720	132.79	168.97
	aug-cc-pVTZ[c]	val	1.0748	1.3080	1.1764	131.68	168.54
	aug-cc-pVQZ[c]	val	1.0734	1.3035	1.1730	132.58	168.84
	aug-cc-pV5Z[a]	val	1.0729	1.3023	1.1722	132.75	168.95
	cc-pCVQZ[c]	all	1.0709	1.2975	1.1710	134.10	169.30
	aug-cc-pCVQZ[a]	all	1.0713	1.2981	1.1713	133.82	169.20
c∼CCSDT(Q)	CBS[a]	all	1.0710	1.2977	1.1712	133.70	169.20

[a] This research. [b] Reference 29, using an unrestricted reference wave function. [c] Reference 34.

TABLE 4: Equilibrium Geometries (Å and deg) for the $^2\Pi$ Renner−Teller State of HCCO

method	AO basis	electrons correlated	r(HC)	r(CC)	r(CO)
CCSD	cc-pVQZ[a]	val	1.0597	1.2585	1.1767
	cc-pV5Z[a]	val	1.0595	1.2579	1.1761
	aug-cc-pVQZ[a]	val	1.0599	1.2588	1.1771
	aug-cc-pV5Z[a]	val	1.0595	1.2580	1.1761
CCSD(T)	cc-pVTZ[b]	val	1.0560	1.2609	1.1847
	cc-pVTZ[c]	val	1.0617	1.2653	1.1895
	cc-pVQZ[c]	val	1.0616	1.2628	1.1856
	cc-pV5Z[a]	val	1.0614	1.2621	1.1850
	aug-cc-pVTZ[c]	val	1.0625	1.2659	1.1901
	aug-cc-pVQZ[c]	val	1.0619	1.2631	1.1861
	aug-cc-pV5Z[a]	val	1.0615	1.2623	1.1852
	cc-pCVQZ[c]	all	1.0604	1.2600	1.1834
	cc-pCV5Z[a]	all	1.0601	1.2593	1.1828
	aug-cc-pCVQZ[a]	all	1.0606	1.2603	1.1839
c∼CCSDT(Q)	CBS[a]	all	1.0601	1.2595	1.1835

[a] This research. [b] Reference 29, using an unrestricted reference wave function. [c] Reference 34.

TABLE 5: Rotational Constants and Quartic Centrifugal Distortion Constants (MHz) for the Ketenyl Radical HCCO and Its Deuterated Isotopologue DCCO

	CCSD(T)/ aug-cc-pCVQZ		c∼CCSDT(Q)/ CBS		experiment[a]
	equilibrium	zero-point	equilibrium	zero-point[b]	
			HCCO		
A	1009756	1191253	1005939	1187436	1243000(45000)
B	10924	10885	10930	10891	10896.788(41)
C	10807	10756	10812	10761	10766.466(39)
D_N	0.003741				0.003861(21)
D_{NK}	0.2537				0.2376(26)
D_K	11046				18480(1200)
			DCCO		
A	630614	719027	627912	716325	652100(3600)
B	9945	9910	9951	9916	9926.8008(104)
C	9790	9743	9796	9749	9755.2316(126)
D_N	0.003453				0.0035088(34)
D_{NK}	−1.6621				−1.6724(123)
D_K	4576				5000(fixed)

[a] Reference 15. [b] Based on the c∼CCSDT(Q)/CBS r_e structure and CCSD(T)/aug-cc-pCVQZ α_i constants.

exception of A_0, which exhibits a 4% deviation; the large error bars on the experimental values indicate that such comparisons should be made with caution. Similar trends are observed for the deuterated isotopologue, with the A_0 value from theory lying above that from experiment, in contrast to the HCCO trends.

Some nice results are obtained by zero-point-correcting our c∼CCSDT(Q)/CBS equilibrium rotational constants with AE-CCSD(T)/aug-cc-pCVQZ vibration−rotation interaction constants (cf Table 5). This brings all rotational constants closer to the experimentally observed values for both HCCO and DCCO, with the exception of A_0 for HCCO, for which large experimental error bars are assigned. The absolute % differences between the zero-point c∼CCSDT(Q)/CBS and experimental values for B_0(HCCO), C_0(HCCO), B_0(DCCO), and C_0(DCCO) are 0.05, 0.05, 0.1, and 0.06%, respectively, which is a spectacular level of agreement.

At the CCSD(T)/aug-cc-pCVQZ level, most of the harmonic vibrational frequencies for the $^2A''$ ground state are significantly lower than those computed previously by Szalay et al.,[36] except in the case of the CCH bending mode. In addition to computing harmonic vibrational frequencies, Szalay and co-workers reported fundamental vibrational frequencies for the parent HCCO isotopologue which were derived from a partial CCSD(T)/cc-pVTZ force field and are given in footnote *c* of Table 8. As with the harmonic vibrational frequencies, the fundamental vibrational frequencies from this work are lower than those reported by Szalay et al. Our (ν_1, ν_2, ν_5) values of (3212, 2025, 483) cm^{-1} are in reasonable agreement with those obtained experimentally[17,47,48] (3232, 2023, 494) cm^{-1}. Fermi resonances did not prove to be a problem for this molecule as no $2\omega_i - \omega_j$ or $\omega_i + \omega_j - \omega_k$ differences smaller than 48 cm^{-1} were encountered. The full CCSD(T)/aug-cc-pCVQZ quartic force field of HCCO in internal coordinates is provided as Supporting Information.

Finally, the focal point analysis for the barrier to linearity of HCCO is laid out in Table 9. The CCSD(T) relative energies are converged to within 0.01 kcal mol^{-1} with an aug-cc-pVQZ basis set, which means that the focal point extrapolation has accomplished its first objective, recovering basis set errors. This

TABLE 6: Vibration−Rotation Interaction Constants α_i (MHz) for HCCO, Derived from the All-Electron CCSD(T)/ aug-cc-pCVQZ Anharmonic Force Field[a]

	HCCO	DCCO	H^{13}CCO	HC^{13}CO	HCC^{18}O
α_1^A	115900	69252	112122	114491	115780
α_2^A	12387	−2366	9914	11428	17898
α_3^A	48776	25659	48117	49196	44159
α_1^B	12.86	5.13	12.86	12.80	11.87
α_2^B	74.77	66.31	71.95	72.01	70.99
α_3^B	28.42	19.61	27.61	28.30	26.38
α_4^B	−8.63	−2.46	−11.87	−2.97	−6.24
α_5^B	−33.37	−20.06	−31.36	−29.92	−28.63
α_6^B	6.36	4.32	6.48	−0.54	1.50
α_1^C	25.60	21.35	24.73	25.60	23.38
α_2^C	74.44	63.53	71.41	71.65	71.26
α_3^C	33.31	25.33	32.26	33.31	30.37
α_4^C	−5.82	2.10	−8.54	−3.36	−4.86
α_5^C	5.85	−32.80	5.88	4.44	5.07
α_6^C	−36.36	11.69	−34.63	−35.44	−34.24

[a] The quasilinearity of HCCO renders the α_4^A, α_5^A, and α_6^A values from VPT2 unreliable, and thus, these constants are not reported here.

TABLE 7: Vibrational Anharmonicity Constants x_{ij} (in cm^{-1}) for Selected Isotopologues of the Ketenyl Radical, Computed at the AE-CCSD(T)/aug-cc-pCVQZ Level of Theory

	HCCO	DCCO	H^{13}CCO	HC^{13}CO	HCC^{18}O
x_{11}	−63.24	−34.34	−62.75	−63.25	−63.24
x_{21}	−1.79	−8.16	−2.51	−3.20	−4.25
x_{22}	−14.22	−13.80	−14.30	−13.44	−13.67
x_{31}	−6.27	−3.30	−7.47	−8.10	−7.02
x_{32}	−11.69	−10.24	−10.48	−8.02	−10.65
x_{33}	−4.68	−5.73	−4.54	−4.78	−4.16
x_{41}	11.15	6.37	9.87	13.30	12.10
x_{42}	−2.98	−6.66	−4.44	−0.17	−1.32
x_{43}	12.00	18.09	14.78	7.76	13.79
x_{44}	−11.34	−7.86	−10.16	−14.75	−13.52
x_{51}	0.08	−2.73	0.66	−2.20	−0.89
x_{52}	1.25	−9.87	0.96	−0.09	1.41
x_{53}	4.51	6.53	5.61	3.75	4.28
x_{54}	−39.48	33.47	−39.13	−37.43	−39.66
x_{55}	−11.22	−0.62	−12.57	−7.50	−9.59
x_{61}	−3.84	7.13	−3.81	−3.83	−3.82
x_{62}	−9.51	−0.96	−9.38	−8.79	−9.45
x_{63}	7.88	3.56	8.89	6.17	8.87
x_{64}	40.04	−26.26	41.41	32.33	37.18
x_{65}	22.69	4.95	20.13	29.88	25.45
x_{66}	−1.69	−9.71	−1.95	−1.36	−1.89

TABLE 8: Harmonic and Fundamental Vibrational Frequencies (cm^{-1}) Computed for the $^2A''$ and Linear $^2\Pi$ Structures of HCCO at the AE-CCSD(T)/aug-cc-pCVQZ Level of Theory

			$^2A''$			$^2\Pi$
mode (sym.)[a]	description	TED[b]	ω	ν[c]	Expt.	ω
$\nu_1(a')$	C−H stretch	$S_1(99)$	3339	3212	3232[d]	3463
$\nu_2(a')$	C−O stretch	$S_3(67) - S_2(31)$	2066	2025	2023[e]	2083
$\nu_3(a')$	C−C stretch	$S_2(67) + S_3(33)$	1235	1229		1289
$\nu_4(a')$	CCO bend	$S_5(85) + S_4(14)$	563	550		556
$\nu_5(a')$	HCC bend	$S_4(84) - S_5(15)$	511	483	494[f]	511
$\nu_6(a'')$	torsion	$S_6(100)$	493	519	528	405
						397i

[a] Symmetry assignments are made for the $^2A''$ ground state, with the analogous linear harmonic frequencies shown for comparison. [b] The total energy distribution (TED)[134,135] quantity $S_x(p)$ is the percentage p contribution to the total energy (kinetic and potential) of each vibrational mode from the internal coordinate x (defined in the text). Only contributions greater than 3% are shown, and the sign is representative of the relative phase of each internal coordinate in the normal-mode eigenvector. [c] This work, AE-CCSD(T)/aug-cc-pCVQZ VPT2 results. Corresponding VPT2 results from a partial CCSD(T)/cc-pVTZ quartic force field (ref 36) are (3239, 2038, 1238, 569, 472, 528 cm^{-1}). [d] Reference 48. [e] Reference 47. [f] Reference 17.

lack of basis set sensitivity is in stark contrast to the geometric parameters (cf Tables 3 and 4). The fact that the geometries are highly basis set dependent and the energies are not further highlights the shallow potential associated with the bending mode. The CCSDT correction to the CCSD(T) value is identical for the aug-cc-pVTZ and aug-cc-pVDZ basis sets, which corroborates the implicit assumption of transferability of the high-order corrections between basis sets. The introduction of perturbative quadruples changes the computed barrier height by only 0.1 kcal mol^{-1}, indicating excellent convergence toward the full CI limit. The performance of ZAPT2 theory is noteworthy; the decrease in the barrier to linearity upon the introduction of coupled cluster with singles and doubles is largely canceled by the increase introduced by the higher-order correlation effects.

The focal point limit for the barrier height in the valence-only determination was 2.08 kcal mol^{-1}, while the core correlation correction, found using eq 8, lowered this barrier by a sizable 0.23 kcal mol^{-1}. Since the UCCSDT and ROCCSDT barrier heights differ by only 0.003 kcal mol^{-1}, no significant error is expected from the small amount of spin contamination present in the UCCSDT(Q) wave function. The small post-CCSDT correction of 0.10 kcal mol^{-1} demonstrates excellent convergence toward the full CI limit. Considerations of relativistic effects and the diagonal Born−Oppenheimer correction affect the relative energies by less than 0.1 kcal mol^{-1}, yielding a total classical barrier to linearity of 1.8 ± 0.1 kcal mol^{-1} or 630 ± 30 cm^{-1}. For the sake of experimental comparison, this vibrationless barrier should be corrected for zero-point effects in a manner consistent with the type of experiment in question. Using the harmonic vibrational frequencies shown in Table 8, we compute a standard harmonic zero-point correction of +50 cm^{-1} to the barrier, increasing it to 680 ± 30 cm^{-1}.

In analyzing their high-resolution microwave spectrum, Endo and Hirota[15] provided a tentative estimate of the barrier to linearity. The a-axis spin rotation interaction constant ε_{aa} and the corresponding rotational constant A can be related[15,130] to the excitation energy ΔE to the lowest electronic excited state through the simple formula

$$\Delta E = -\left(\frac{4A}{\varepsilon_{aa}}\right)A_{SO} \tag{9}$$

whose right-hand side is determined from the microwave spectrum, with the exception of the spin−orbit coupling constant A_{SO}. The lowest excited electronic state is the $^2A'$ state, which becomes degenerate with the $^2A''$ ground state at linearity in the absence of zero-field splitting. Given that the minimum on the $^2A'$ potential energy surface is located at linearity, the barrier to linearity can be estimated from the excitation energy, ΔE, of the $^2A'$ state. Endo and Hirota assumed the spin−orbit coupling to be bound by either that of atomic carbon (27.1 cm^{-1}) or atomic oxygen (158.5 cm^{-1}), depending on where the unpaired electron was localized. This intuitive approach, coupled with eq 9, yielded two values of 540 and 3200 cm^{-1} for the barrier to linearity. Szalay and Blandeau[31] refined this estimate by computing the spin−orbit coupling constant for the $^2\Pi$ state of HCCO, which, at first order, is given by[131]

$$A_{SO} = 2\langle \Psi_{^2\Pi_x} | \hat{H}_{SO} | \Psi_{^2\Pi_y} \rangle \tag{10}$$

The resulting spin–orbit coupling constant, computed using spin−orbit configuration interaction theory with a relativistic effective core potential, is 59 cm^{-1}, which yields an excitation energy of 1175 cm^{-1} when inserted into eq 9. Such a spin−orbit coupling constant is consistent with the slightly delocalized nature of the electron, which is predominantly localized on the

TABLE 9: Valence Focal Point Analysis of the Barrier to Linearity (in kcal mol^{-1}) for HCCO[a]

basis set	ΔE_e[ROHF]	δ[ZAPT2]	δ[CCSD]	δ[CCSD(T)]	δ[CCSDT]	δ[CCSDT(Q)]	ΔE_e[CCSDT(Q)]
aug-cc-pVDZ	+1.85	+1.71	−0.50	+0.68	+0.07	+0.10	[+3.91]
aug-cc-pVTZ	+1.08	+1.21	−0.60	+0.61	+0.07	[+0.10]	[+2.47]
aug-cc-pVQZ	+1.08	+0.96	−0.61	+0.60	[+0.07]	[+0.10]	[+2.20]
aug-cc-pV5Z	+1.07	+0.89	−0.59	+0.60	[+0.07]	[+0.10]	[+2.14]
aug-cc-pV6Z	+1.06	+0.85	−0.58	+0.60	[+0.07]	[+0.10]	[+2.10]
∞	[+1.06]	[+0.81]	[−0.56]	[+0.60]	[+0.07]	[+0.10]	**[+2.08]**
ΔE_e(final) = ΔE_e[CBS CCSDT(Q)] + Δ_{core}[CCSD(T)/aug-cc-pCVQZ] + Δ_{rel}[CCSD(T)/aug-cc-pCVTZ] + Δ_{DBOC}[HF/aug-cc-pVTZ] = 2.08 − 0.23 + 0.04 − 0.10 = **1.79 kcal mol^{-1}**							
fit function	$a + be^{-cX}$	$a + bX^{-3}$	$a + bX^{-3}$	$a + bX^{-3}$	additive	additive	
points (X)	4,5,6	5,6	5,6	5,6			

[a] The symbol δ denotes the increment in the relative energy (ΔE_e) with respect to the preceding level of theory in the hierarchy ROHF → ZAPT2 → CCSD → CCSD(T) → CCSDT → CCSDT(Q). Square brackets signify results obtained from basis set extrapolations or additivity assumptions. Final predictions are boldfaced.

carbon atom. However, the direct interpretation of ΔE in eq 9 as the barrier to linearity is questionable. Implicit to the derivation of eq 9 is the assumption that the matrix element $|\langle \Psi_{^2A''} | L_a | \Psi_{^2A'} \rangle|^2$ is unity and that only the $^2A'$ state contributes to the spin−rotation coupling at second order. For many molecules, these conditions are not fulfilled, and the resultant ΔE can be overestimated by as much as a factor of 3, as demonstrated in the tabulations of Hirota on page 191 of ref 130.

An alternative experimental determination of the barrier to linearity was performed by Schäfer-Bung and co-workers,[34] who compared simulated photoelectron spectra with the experimental spectrum of $HCCO^-$. By considering various ab initio geometries and by systematically tuning the barrier height assumed within their theoretical models, a range of 700−900 cm^{-1} was deduced for the barrier to linearity. The lower end of this range is compatible with our theoretical value. These experimental values are shown, along with various theoretical predictions, in Table 1 for comparison purposes.

Conclusions

In this study, the geometry and barrier to linearity for the HCCO radical have been determined by high-level ab initio quantum chemical methods. A full quartic force field has also been computed to determine HCCO fundamental frequencies that agree satisfactorily with experiment; the resulting constants reported herein can be used to predict myriad spectroscopic properties accurately and will be of utility in the experimental characterization of HCCO isotopologues.

The geometry of the $^2A''$ ground state is known to be sensitive to the theoretical method used, leading us to define an approximation to CCSDT(Q) theory at the complete basis set limit. This composite level of theory produced geometries and frequencies in excellent accord with experimental values for the constituent diatomic molecules, CH and CO, relying on cancellation of basis set and correlation errors to a lesser extent than CCSD(T)/aug-cc-pCVQZ theory. The results for these diatomics and for the HCCO molecule itself indicate that the composite CCSDT(Q) approach offers a more tractable alternative to its more expensive CCSDTQ counterpart.

The focal point extrapolation procedure, including correlation contributions up to CCSDT(Q) and a number of auxiliary effects, yielded a classical barrier to linearity for the ketenyl radical of 630 ± 30 cm^{-1}, which increases to 680 ± 30 cm^{-1} with the inclusion of the usual zero-point vibrational correction. This result is broadly consistent with the values suggested from the spectroscopic investigations of Endo and Hirota[15] (540 or 3200 cm^{-1}) and the Neumark group[34] (800 ± 100 cm^{-1}).

Acknowledgment. This research was supported by the U.S. Department of Energy, Office of Basic Energy Sciences, Combustion Program (Grant No. DE-FG02-00ER14748) and used resources of the National Energy Research Scientific Computing Center, which is supported by the Office of Science of the U.S. Department of Energy under Contract No. DE-AC02-05CH11231.

Supporting Information Available: The full CCSD(T)/aug-cc-pCVQZ quartic force field, in internal coordinates, for the $^2A''$ ground state of HCCO. This material is available free of charge via the Internet at http://pubs.acs.org.

References and Notes

(1) Warnatz, J. In *Combustion Chemistry*; Gardiner, W. C., Ed.; Springer-Verlag: New York, 1984; p 288.
(2) Cooper, D. L. *Astrophys. J.* **1983**, *265*, 808.
(3) Turner, B. E.; Sears, T. J. *Astrophys. J.* **1989**, *340*, 900.
(4) Jones, I. T. N.; Bayes, K. D. *J. Am. Chem. Soc.* **1972**, *94*, 6869.
(5) Vinckier, C.; Schaekers, M.; Peeters, J. *J. Phys. Chem.* **1985**, *89*, 508.
(6) Jacox, M. E.; Olson, W. B. *J. Chem. Phys.* **1987**, *86*, 3134.
(7) Boullart, W.; Peeters, J. *J. Phys. Chem.* **1992**, *96*, 9810.
(8) Murray, K. K.; Unfried, K. G.; Glass, G. P.; Curl, R. F. *Chem. Phys. Lett.* **1992**, *192*, 512.
(9) Boullart, W.; Nguyen, M. T.; Peeters, J. *J. Phys. Chem.* **1994**, *98*, 8036.
(10) Peeters, J.; Langhans, I.; Boullart, W.; Nguyen, M. T.; Devriendt, K. *J. Phys. Chem.* **1994**, *98*, 11988.
(11) Peeters, J.; Boullart, W.; Devriendt, K. *J. Phys. Chem.* **1995**, *99*, 3583.
(12) Carl, S. A.; Sun, Q.; Peeters, J. *J. Chem. Phys.* **2001**, *114*, 10332.
(13) Oakes, J. M.; Jones, M. E.; Bierbaum, V. M.; Ellison, G. B. *J. Phys. Chem.* **1983**, *87*, 4810.
(14) Krishnamachari, S. L. N. G.; Venkatasubramanian, R. *Pramana* **1984**, *23*, 321.
(15) Endo, Y.; Hirota, E. *J. Chem. Phys.* **1987**, *86*, 4319.
(16) Hanratty, M. A.; Nelson, H. H. *J. Chem. Phys.* **1990**, *92*, 814.
(17) Unfried, K. G.; Curl, R. F. *J. Mol. Spectrosc.* **1991**, *150*, 86.
(18) Unfried, K. G.; Glass, G. P.; Curl, R. F. *Chem. Phys. Lett.* **1991**, *177*, 33.
(19) Ohshima, Y.; Endo, Y. *J. Mol. Spectrosc.* **1993**, *159*, 458.
(20) Mordaunt, D. H.; Osborn, D. L.; Choi, H.; Bise, R. T.; Neumark, D. M. *J. Chem. Phys.* **1996**, *105*, 6078.
(21) Brock, L. R.; Mischler, B.; Rohlfing, E. A. *J. Chem. Phys.* **1999**, *110*, 6773.
(22) Jerosimić, S. V. *J. Mol. Spectrosc.* **2007**, *242*, 139.
(23) Harding, L. B. *J. Phys. Chem.* **1981**, *85*, 10.
(24) Harding, L. B.; Wagner, A. F. *J. Phys. Chem.* **1986**, *90*, 2974.
(25) Goddard, J. D. *Chem. Phys. Lett.* **1989**, *154*, 387.
(26) Szalay, P. G.; Stanton, J. F.; Bartlett, R. J. *Chem. Phys. Lett.* **1992**, *193*, 573.
(27) Hu, C. H.; Schaefer, H. F.; Hou, Z. L.; Bayes, K. D. *J. Am. Chem. Soc.* **1993**, *115*, 6904.
(28) Nguyen, M. T.; Boullart, W.; Peeters, J. *J. Phys. Chem.* **1994**, *98*, 8030.
(29) Szalay, P. G.; Fogarasi, G.; Nemes, L. *Chem. Phys. Lett.* **1996**, *263*, 91.
(30) Yarkony, D. R. *J. Phys. Chem.* **1996**, *100*, 17439.
(31) Szalay, P. G.; Blaudeau, J. P. *J. Chem. Phys.* **1997**, *106*, 436.
(32) Yamaguchi, Y.; Rienstra-Kiracofe, J. C.; Stephens, J. C.; Schaefer, H. F. *Chem. Phys. Lett.* **1998**, *291*, 509.
(33) Schäfer, B.; Perić, M.; Engels, B. *J. Chem. Phys.* **1999**, *110*, 7802.
(34) Schäfer-Bung, B.; Engels, B.; Taylor, T. R.; Neumark, D. M.; Botschwina, P.; Perić, M. *J. Chem. Phys.* **2001**, *115*, 1777.
(35) Sattelmeyer, K. W.; Yamaguchi, Y.; Schaefer, H. F. *Chem. Phys. Lett.* **2004**, *383*, 266.
(36) Szalay, P. G.; Tajti, A.; Stanton, J. F. *Mol. Phys.* **2005**, *103*, 2159.
(37) Fenimore, C. P.; Jones, G. W. *J. Chem. Phys.* **1963**, *39*, 1514.
(38) Wetmore, R. W.; Schaefer, H. F. *J. Chem. Phys.* **1978**, *69*, 1648.
(39) Michael, J. V.; Wagner, A. F. *J. Phys. Chem.* **1990**, *94*, 2453.
(40) Chikan, V.; Leone, S. R. *J. Phys. Chem. A* **2005**, *109*, 2525.
(41) Casavecchia, P.; Leonori, F.; Balucani, N.; Petrucci, R.; Capozza, G.; Segoloni, E. *Phys. Chem. Chem. Phys.* **2009**, *11*, 46.
(42) Golden, D. M. *Proc. Combust. Inst.* **2000**, *28*, 2383.
(43) Smoot, L. D.; Hill, S. C.; Xu, H. *Prog. Energy Combust. Sci.* **1998**, *24*, 385.
(44) Glarborg, P.; Alzueta, M. U.; Dam-Johansen, K.; Miller, J. A. *Combust. Flame* **1998**, *115*, 1.
(45) Hien, M. T.; Nguyen, T. L.; Carl, S. A.; Nguyen, M. T. *Chem. Phys. Lett.* **2005**, *416*, 199.
(46) Meyer, J. P.; Hershberger, J. F. *J. Phys. Chem. A* **2005**, *109*, 4772.
(47) Brock, L. R.; Mischler, B.; Rohlfing, E. A.; Bise, R. T.; Neumark, D. M. *J. Chem. Phys.* **1997**, *107*, 665.
(48) Wilhelm, M. J.; McNavage, W.; Groller, R.; Dai, H. L. *J. Chem. Phys.* **2008**, *128*, 8.
(49) Krisch, M. J.; Miller, J. L.; Butler, L. J.; Su, H.; Bersohn, R.; Shu, J. *J. Chem. Phys.* **2003**, *119*, 176.
(50) Lee, T. J.; Fox, D. J.; Schaefer, H. F.; Pitzer, R. M. *J. Chem. Phys.* **1984**, *81*, 356.
(51) Devriendt, K.; van Look, H.; Ceursters, B.; Peeters, J. *Chem. Phys. Lett.* **1996**, *261*, 450.
(52) Devriendt, K.; Peeters, J. *J. Phys. Chem. A* **1997**, *101*, 2546.
(53) Chikan, V.; Nizamov, B.; Leone, S. R. *J. Phys. Chem. A* **2004**, *108*, 10770.
(54) Roothaan, C. C. J. *Rev. Mod. Phys.* **1960**, *32*, 179.
(55) Lee, T. J.; Jayatilaka, D. *Chem. Phys. Lett.* **1993**, *201*, 1.
(56) Rittby, M.; Bartlett, R. J. *J. Phys. Chem.* **1988**, *92*, 3033.

(57) Stanton, J. F.; Gauss, J.; Watts, J. D.; Bartlett, R. J. *J. Chem. Phys.* **1991**, *94*, 4334.
(58) Hampel, C.; Peterson, K. A.; Werner, H.-J. *Chem. Phys. Lett.* **1992**, *190*, 1.
(59) Watts, J. D.; Gauss, J.; Bartlett, R. J. *Chem. Phys. Lett.* **1992**, *200*, 1.
(60) Raghavachari, K.; Trucks, G. W.; Pople, J. A.; Head-Gordon, M. *Chem. Phys. Lett.* **1989**, *157*, 479.
(61) Knowles, P. J.; Hampel, C.; Werner, H.-J. *J. Chem. Phys.* **1993**, *99*, 5219.
(62) Watts, J. D.; Gauss, J.; Bartlett, R. J. *J. Chem. Phys.* **1993**, *98*, 8718.
(63) Stanton, J. F. *Chem. Phys. Lett.* **1997**, *281*, 130.
(64) Noga, J.; Bartlett, R. J. *J. Chem. Phys.* **1987**, *86*, 7041.
(65) Scuseria, G. E.; Schaefer, H. F. *Chem. Phys. Lett.* **1988**, *152*, 382.
(66) Watts, J. D.; Bartlett, R. J. *J. Chem. Phys.* **1990**, *93*, 6104.
(67) Gauss, J.; Stanton, J. F. *J. Chem. Phys.* **2002**, *116*, 1773.
(68) Bomble, Y. J.; Stanton, J. F.; Kállay, M.; Gauss, J. *J. Chem. Phys.* **2005**, *123*, 054101.
(69) Kállay, M.; Gauss, J. *J. Chem. Phys.* **2005**, *123*, 214105.
(70) Kendall, R. A.; Dunning, T. H., Jr.; Harrison, R. J. *J. Chem. Phys.* **1992**, *96*, 6796.
(71) Woon, D. E.; Dunning, T. H., Jr. *J. Chem. Phys.* **1994**, *100*, 2975.
(72) van Mourik, T.; Wilson, A. K.; Dunning, T. H., Jr. *Mol. Phys.* **1999**, *96*, 529.
(73) Dunning, T. H., Jr. *J. Chem. Phys.* **1989**, *90*, 1007.
(74) Woon, D. E.; Dunning, T. H., Jr. *J. Chem. Phys.* **1995**, *103*, 4572.
(75) Gauss, J.; Stanton, J. F.; Bartlett, R. J. *J. Chem. Phys.* **1991**, *95*, 2623.
(76) Stanton, J. F.; Gauss, J. *Int. Rev. Phys. Chem.* **2000**, *19*, 61.
(77) East, A. L. L.; Johnson, C. S.; Allen, W. D. *J. Chem. Phys.* **1993**, *98*, 1299.
(78) Nielsen, H. H. *Rev. Mod. Phys.* **1951**, *23*, 90.
(79) Mills, I. M. In *Molecular Spectroscopy: Modern Research*; Rao, K. N., Mathews, C. W., Eds.; Academic Press: New York, 1972; p 115.
(80) Watson, J. K. G. In *Vibrational Spectra and Structure*; Durig, J. R., Ed.; Elsevier: Amsterdam, The Netherlands, 1972; Vol. 6, p 1.
(81) Papoušek, D.; Aliev, M. R. *Molecular Vibrational−Rotation Spectra*; Elsevier: Amsterdam, The Netherlands, 1982.
(82) Clabo, D. A., Jr.; Allen, W. D.; Remington, R. B.; Yamaguchi, Y.; Schaefer, H. F. *Chem. Phys.* **1988**, *123*, 187.
(83) Allen, W. D; Yamaguchi, Y.; Császár, A. G.; Clabo, D. A., Jr.; Remington, R. B.; Schaefer, H. F. *Chem. Phys.* **1990**, *145*, 427.
(84) Aarset, K.; Császár, A. G.; Sibert, E. L.; Allen, W. D.; Schaefer, H. F.; Klopper, W.; Noga, J. *J. Chem. Phys.* **2000**, *112*, 4053.
(85) *MATHEMATICA*; Wolfram Research, Inc.: Champaign, IL.
(86) Allen, W. D. *INTDIF2005*, an abstract program for Mathematica to perform general numerical differentiations to high orders of electronic structure data; 2005.
(87) DeKock, R. L.; McGuire, M. J.; Piecuch, P.; Allen, W. D.; Schaefer, H. F.; Kowalski, K.; Kucharski, S. A.; Musiał, M.; Bonner, A. R.; Spronk, S. A.; Lawson, D. B.; Laursen, S. L. *J. Phys. Chem. A* **2004**, *108*, 2893.
(88) Allen, W. D.; et al. *INTDER2005*; a general program which performs various vibrational analyses and higher-order nonlinear transformations among force field representation; 2005.
(89) Allen, W. D.; Császár, A. G. *J. Chem. Phys.* **1993**, *98*, 2983.
(90) Allen, W. D.; Császár, A. G.; Szalay, V.; Mills, I. M. *Mol. Phys.* **1996**, *89*, 1213.
(91) Sarka, K.; Demaison, J. In *Computational Molecular Spectroscopy*; Jensen, P., Bunker, P. R., Eds.; Wiley: Chichester, U.K., 2000; p 255.
(92) Simmonett, A. C.; Evangelista, F. A.; Allen, W. D.; Schaefer, H. F. *J. Chem. Phys.* **2007**, *127*, 014306.
(93) Yamaguchi, Y.; Schaefer, H. F. *ANHARM*, a FORTRAN program written for VPT2 analysis; Center for Computational Chemistry, University of Georgia: Athens, GA.
(94) Karton, A.; Martin, J. M. L. *Theor. Chem. Acc.* **2006**, *115*, 330.
(95) Helgaker, T.; Klopper, W.; Koch, H.; Noga, J. *J. Chem. Phys.* **1997**, *106*, 9639.
(96) Ruden, T. A.; Helgaker, T.; Jørgensen, P.; Olsen, J. *J. Chem. Phys.* **2004**, *121*, 5874.
(97) Hirata, S.; Yanai, T.; de Jong, W. A.; Nakajima, T.; Hirao, K. *J. Chem. Phys.* **2004**, *120*, 3297.
(98) Heckert, M.; Kállay, M.; Gauss, J. *Mol. Phys.* **2005**, *103*, 2109.
(99) Heckert, M.; Kállay, M.; Tew, D. P.; Klopper, W.; Gauss, J. *J. Chem. Phys.* **2006**, *125*, 044108.
(100) Zhang, X.; Maccarone, A. T.; Nimlos, M. R.; Kato, S.; Bierbaum, V. M.; Ellison, G. B.; Ruscic, B.; Simmonett, A. C.; Allen, W. D.; Schaefer, H. F. *J. Chem. Phys.* **2007**, *126*, 044312.
(101) Crawford, T. D.; Sherrill, C. D.; Valeev, E. F.; Fermann, J. T.; King, R. A.; Leininger, M. L.; Brown, S. T.; Janssen, C. L.; Seidl, E. T.; Kenny, J. P.; Allen, W. D. *J. Comput. Chem.* **2007**, *28*, 1610.
(102) East, A. L. L.; Allen, W. D. *J. Chem. Phys.* **1993**, *99*, 4638.
(103) Császár, A. G.; Allen, W. D.; Schaefer, H. F. *J. Chem. Phys.* **1998**, *108*, 9751.
(104) Gonzales, J. M.; Pak, C.; Cox, R. S.; Allen, W. D.; Schaefer, H. F.; Császár, A. G.; Tarczay, G. *Chem.—Eur. J.* **2003**, *9*, 2173.
(105) Kenny, J. P.; Allen, W. D.; Schaefer, H. F. *J. Chem. Phys.* **2003**, *118*, 7353.
(106) Schuurman, M. S.; Muir, S. R.; Allen, W. D.; Schaefer, H. F. *J. Chem. Phys.* **2004**, *120*, 11586.
(107) Feller, D. *J. Chem. Phys.* **1993**, *98*, 7059.
(108) Kállay, M.; Gauss, J. *J. Chem. Phys.* **2008**, *129*, 144101.
(109) Janssen, C. L.; Nielsen, I. B.; Leininger, M. L.; Valeev, E. F.; Kenny, J. P.; Seidl, E. T. *The Massively Parallel Quantum Chemistry Program (MPQC), 2.3.4*; Sandia National Laboratories: Livermore, CA, 2008; see http://www.mpqc.org.
(110) Nielsen, I. M. B.; Seidl, E. T. *J. Comput. Chem.* **1995**, *16*, 1301.
(111) Knowles, P. J.; Andrews, J. S.; Amos, R. D.; Handy, N. C.; Pople, J. A. *Chem. Phys. Lett.* **1991**, *186*, 130.
(112) Lauderdale, W. J.; Stanton, J. F.; Gauss, J.; Watts, J. D.; Bartlett, R. J. *Chem. Phys. Lett.* **1991**, *187*, 21.
(113) Lee, T. J.; Rendell, A. P.; Dyall, K. G.; Jayatilaka, D. *J. Chem. Phys.* **1994**, *100*, 7400.
(114) Crawford, T. D.; Schaefer, H. F.; Lee, T. J. *J. Chem. Phys.* **1996**, *105*, 1060.
(115) Wheeler, S. E.; Allen, W. D.; Schaefer, H. F. *J. Chem. Phys.* **2008**, *128*, 074107.
(116) Werner, H.-J.; Knowles, P. J.; Lindh, R.; Manby, F. R.; Schütz, M.; et al. *MOLPRO*, version 2006.1, a package of ab initio programs; 2006; see http://www.molpro.net.
(117) Stanton, J. F.; Gauss, J.; Watts, J. D.; Lauderdale, W. J.; Bartlett, R. J. *Int. J. Quantum Chem.* **1992**, *44* (S26), 879.
(118) *ACESII*; Stanton, J. F.; Gauss, J.; Watts, J. D.; Szalay, P. G.; Bartlett, R. J. with contributions from Auer, A. A.; Bernholdt, D. E.; Christiansen, O.; Harding, M. E.; Heckert, M.; Heun, O.; Huber, C.; Jonsson, D.; Jusélius, J.; Lauderdale, W. J.; Metzroth, T.; Michauk, C.; O'Neill, D. P.; Price, D. R.; Ruud, K.; Schiffmann, F.; Tajti, A.; Varner, M. E.; Vázquez, J. and the integral packages *MOLECULE* (Almölf, J.; Taylor, P. R.); *PROPS* (Taylor, P. R.); *ABACUS* (Helgaker, T.; Jensen, H. J. Aa.; Jørgensen, P.; Olsen, J.); for the current version, see http://www.aces2.de.
(119) Kállay, M.; Surján, P. *J. Chem. Phys.* **2001**, *115*, 2945.
(120) Sellers, H.; Pulay, P. *Chem. Phys. Lett.* **1984**, *103*, 463.
(121) Handy, N. C.; Yamaguchi, Y.; Schaefer, H. F. *J. Chem. Phys.* **1986**, *84*, 4481.
(122) Valeev, E. F.; Sherrill, C. D. *J. Chem. Phys.* **2003**, *118*, 3921.
(123) Tajti, A.; Szalay, P. G.; Császár, A. G.; Kállay, M.; Gauss, J.; Valeev, E. F.; Flowers, B.; Vazquez, A.; Stanton, J. F. *J. Chem. Phys.* **2004**, *121*, 11599.
(124) Gauss, J.; Tajti, A.; Kállay, M.; Stanton, J. F.; Szalay, P. G. *J. Chem. Phys.* **2006**, *125*, 144111.
(125) Cowan, R. D.; Griffin, D. C. *J. Opt. Soc. Am.* **1976**, *66*, 1010.
(126) Davidson, E. R.; Ishikawa, Y.; Malli, G. L. *Chem. Phys. Lett.* **1981**, *84*, 226.
(127) Bauschlicher, C. W.; Martin, J. M. L.; Taylor, P. R. *J. Phys. Chem. A* **1999**, *103*, 7715.
(128) Tarczay, G.; Császár, A. G.; Klopper, W.; Quiney, H. M. *Mol. Phys.* **2001**, *99*, 1769.
(129) Boese, A. D.; Oren, M.; Atasoylu, O.; Martin, J. M. L.; Kállay, M.; Gauss, J. *J. Chem. Phys.* **2004**, *120*, 4129.
(130) Hirota, E. *High Resolution Spectroscopy of Transient Molecules*; Springer: Heidelberg, Germany, 1985.
(131) Hess, B. A.; Marian, C. M.; Peyerimhoff, S. D. In *Modern Electronic Structure Theory, Part I*; Yarkony, D. R., Ed.; World Scientific: Singapore, 1995; pp 152−278.
(132) Zachwieja, M. *J. Mol. Spectrosc.* **1995**, *170*, 285.
(133) Mantz, A. W.; Maillard, J.-P.; Roh, W. B.; Rao, K. N. *J. Mol. Spectrosc.* **1975**, *57*, 155.
(134) Pulay, P.; Török, F. *Acta Chim. Hung.* **1965**, *44*, 287.
(135) Allen, W. D.; Császár, A. G.; Horner, D. A. *J. Am. Chem. Soc.* **1992**, *114*, 6834.

JP9024365